EPJ Web of Conferences **10**, 00020 (2010)
DOI: 10.1051/epjconf/20101000020

Vector Image Polygon (VIP) limiters in ALE Hydrodynamics

G. Luttwak[1,a] and J. Falcovitz[2]

[1] Rafael, Box 2250, Haifa 31021, Israel
[2] Institute of Mathematics, The Hebrew University of Jerusalem, Israel

Abstract. Recently ([1,2]) we have formulated a new frame invariant monotonicity criterion and slope limiter for vectors and applied it to the Lagrangian phase of the SMG/Q scheme. This Vector Image Polygon/Polyhedron (VIP) limiter was shown to improve symmetry preservation in a set of test problems. In this study we implement the VIP limiter also to the momentum advection phase of the SMQ/Q scheme for (Arbitrary Lagrangian Eulerian) ALE hydrodynamics. The 2D cylindrical Noh problem serves as a test case to demonstrate the effect of the VIP limiter on symmetry preservation.

1 Introduction

Second order Godunov ([3,4]) and several other high resolution schemes use the gradients of the variables to compute the flux terms required in the solution of the conservation laws. In hyperbolic partial differential equations discontinuities may be present or can evolve in time. At these (captured) discontinuities the gradients are not well defined and using them directly can produce unphysical fluctuations in the solution. Therefore such schemes must use flux or slope limiters to prevent monotonicity violations. These limiter schemes were formulated for **scalar** variables. For vectors or tensors the limiters are usually applied separately to each component. Such a procedure is inherently frame dependent and does not preserve the rotational or planar symmetries present in a problem. High resolution techniques were originally developed in one dimension and later have been applied to multi-dimensional problems, mainly by operator splitting [3,4]. More recent works (see [5–7]) consider aspects associated with extending the limiters to multi-dimensional problems, to non-uniform or to unstructured meshes. However the fact that limiting a vector or tensor by its components is in principle wrong has not been addressed.

Recently, ([1,2]) we have proposed a frame invariant monotonicity criterion and limiter aimed specifically at vector variables. Its formulation is based on a convex hull of a VIP (Vector Image Polygon or Polyhedron), and it was applied to the Lagrangian phase of the SMG scheme. The VIP limiter has considerably improved symmetry preservation in several Lagrangian test problems. In the present study we implement the VIP SMG limiter in the advection phase of the SMG scheme. The 2D cylindrical Noh problem was run in ALE mode, serving to assess the performance of the VIP limiter in ALE calculations.

2 VIP monotonicity criterion for vectors

A scalar variable like ρ (density) is termed monotonicity compliant if its value lies in the range spanned by the density in neighboring zones ν. Labeling $\rho_{min} = \min_\nu(\rho_\nu)$ and $\rho_{max} = \max_\nu(\rho_\nu)$ this can be

[a] e-mail: gabilo@rafael.co.il

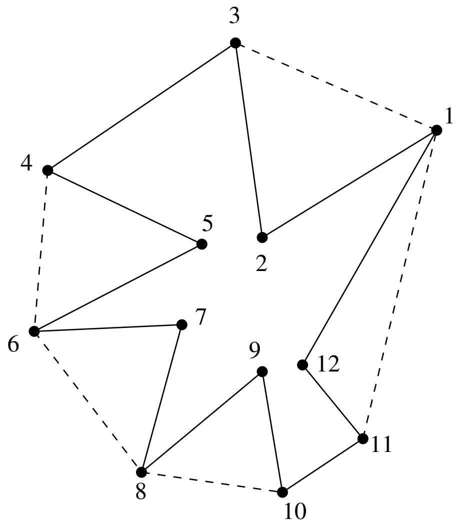

Fig. 1. The Convex hull of points in 2D.

expressed as:

$$[\rho = \alpha\rho_{min} + (1-\alpha)\rho_{max}\ ;\quad 0 \le \alpha \le 1] \tag{1}$$

Searching for a frame invariant criterion to determine if a vector lies in the range spanned by its neighbors, we define the VIP – Vector Image Polygon (or Polyhedron) as the convex hull (CH) of the vector-space points corresponding to the vectors at neighbor zones (or nodes). A vector lying inside the VIP is termed **monotonicity compliant**. Considering a convex hull as in Fig. 1, the original vertices clearly constitute a non-convex (concave) polygon. We **define the convex hull** of a polygon as the ensemble of vectors spanned by the "convex linear combination" of its vertices $\mathbf{v_i}$:

$$[\mathbf{v} = \Sigma\alpha_i\vec{v_i}\ ;\quad 0 \le \alpha_i \le 1\ ,\quad \Sigma\alpha_i = 1]\ , \tag{2}$$

where for a scalar variable this definition reduces to Eq. (1). This concept can be applied to any high resolution scheme requiring flux or slope limiters for vectors or tensors. The slope limiter should limit the gradients in such a way that slope-extrapolated values of the vectors stay inside the VIP. A flux limiter should ensure that the new post-advection values of the vectors also remain inside the corresponding VIP. While the form of a specific VIP based slope or flux limiter will depend on the details of the particular scheme, we believe that the VIP **monotonicity criterion** constitutes the proper (frame-invariant) extension of scalar monotonicity to vectors or tensors. The set-up of the CH for a given polygon is a standard problem in computational geometry [8]. In [1] we describe the CH algorithm used in our SMG code.

3 Lagrangian phase of the SMG/Q scheme

In the Staggered Mesh Godunov SMG/Q scheme [1,2,9,10], the momentum equation is solved over a staggered mesh (Fig. 2). The node-centered velocities are assumed to produce a piecewise linear distribution with possible discontinuities at the in-cell corner zone interfaces (see A in Fig. 3) which separate each pair of edge-neighbor vertices, e.g. $(i, i+1)$ in cell k. Zone centered velocity gradients $(\nabla\mathbf{u})_k$ are calculated from the zone vertices velocities. These gradients, limited to preserve a monotonic velocity (see Ch. 4 below), are then used to compute the velocity jump at A. It is here that the new VIP limiter is applied instead of the previous component-wise limiter. Since zone-centered pressure and density are naturally continuous at A, a simplified "Impact Riemann Problem" (IRP) is solved at A. The resulting pressure p^* acts on the corner zone faces. Integrating the contributions from all corner

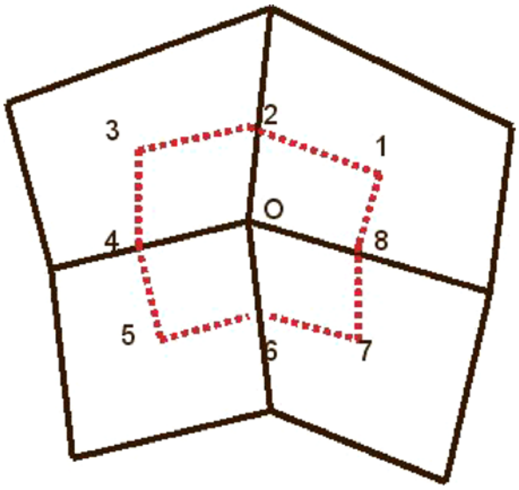

Fig. 2. The SMG momentum control volume.

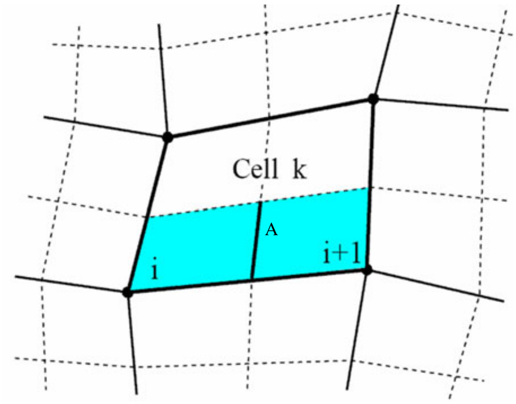

Fig. 3. The SMG scheme.

zone faces surrounding a vertex i, would directly give its time-advanced vertex velocity. Instead, we split this process into two stages: setting $p^* = p_k + (p^* - p_k)$, the contribution of cell pressures p_k is first integrated around vertex i. Then the additional term $Q = p^* - p_k$ is treated as a uniaxial pseudo-viscosity (see also [13]), that exerts forces along the normal to shock direction taken along the edge neighbors velocity difference $\Delta\mathbf{u}_{i,i+1}$. The work done by the Q-forces is used to update the cell internal energy like in "compatible hydrodynamics" [14].

4 The SMG VIP slope-limiter

The VIP limiter is applied in both the Lagrangian and advection phases of the SMG/ALE scheme. The gradient is limited separately along each edge of a cell. Consider a locally Cartesian mesh as in Fig. 4 (the algorithm can be applied to a general connectivity mesh as well). We have to limit the slope between the two edge neighbors (points 1 and 2) in cell k (one of the two cells surrounding the edge $\bar{12}$). Let $\hat{u}_{12}$ and $\hat{r}_{12}$ be unit vectors along the velocity difference $\Delta\mathbf{u}_{12}$ and edge segment $\bar{12}$, respectively. Then:

$$\Delta\mathbf{u}_{12} = \mathbf{u}_2 - \mathbf{u}_1; \quad \hat{u}_{12} = \frac{\Delta\mathbf{u}_{12}}{|\Delta\mathbf{u}_{12}|} \tag{3}$$

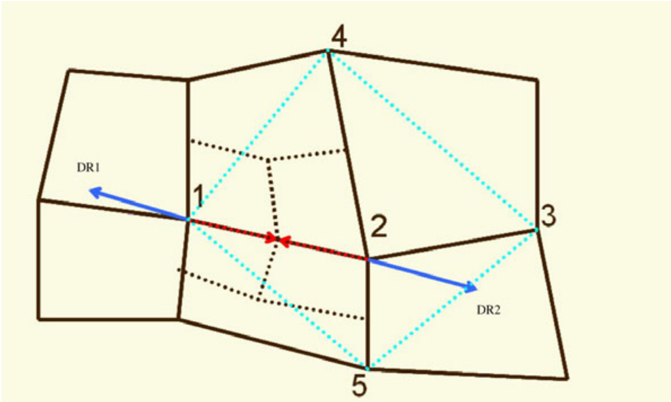

Fig. 4. The SMG VIP Limiter.

$$\Delta \mathbf{r}_{12} = \mathbf{r}_2 - \mathbf{r}_1; \quad \hat{r}_{12} = \frac{\Delta \mathbf{r}_{12}}{|\Delta \mathbf{r}_{12}|} \tag{4}$$

We assume the limited velocity gradient to be along $\hat{u}_{12}$. To limit the slope between points 1 and 2, we extrapolate the node velocities of points 1 and 2 outward along the edge toward the (projected) midpoint of their neighbor segments. For vertex 2 to the (projected) midpoint of $\bar{23}$:

$$\delta \mathbf{r_2} = 0.5(\Delta \mathbf{r_{23}} \cdot \hat{r_{12}})\hat{r_{12}} \tag{5}$$

To get the extrapolated velocity $\mathbf{u}_{2,e}$ we use the cell k centered velocity gradient projected along $\hat{u}_{12}$:

$$\mathbf{u}_{2,e} = \mathbf{u}_2 + \psi_2\left(\left([\nabla \mathbf{u}]_k \cdot \delta \mathbf{r}_2\right) \cdot \hat{u}_{12}\right)\hat{u}_{12} \tag{6}$$

The value of $0 \leq \psi_2 \leq 1$ is chosen so as to keep $\mathbf{u}_{2,e}$ inside the VIP spanned by the edge neighbors of 2 (points 1, 5, 3, 4 in Fig. 4). Likewise, $\mathbf{u}_{1,e}$ is extrapolated from point 1, and ψ_1 is determined so as to keep it inside the VIP corresponding to the edge neighbors of point 1. Finally the velocity jump $[\Delta \mathbf{u}_{12}]$ at the corner zone faces inside cell k separating nodes 1 and 2 (i.e., the IRP data) will be:

$$[\Delta \mathbf{u}_{12}] = \Delta \mathbf{u}_{12} - \Delta \mathbf{u}_{12}^{red} \tag{7}$$

$$\Delta \mathbf{u}_{12}^{red} = \min(\psi_1, \psi_2)\left(\left([\nabla \mathbf{u}]_k \cdot \mathbf{r}_{12}\right) \cdot \hat{u}_{12}\right)\hat{u}_{12} \tag{8}$$

5 The momentum advection

During the advection phase the conservation of momentum (Eq. (9)) is solved over the staggered mesh (Fig. 2).

$$\frac{\mathrm{d}}{\mathrm{d}t}\int_{V_{st}} \rho \mathbf{u} \mathrm{d}V = \int_{\partial V_{st}} \rho \mathbf{u}(\mathbf{u} - \mathbf{u}_g) \cdot \mathrm{d}\mathbf{s} \tag{9}$$

Momentum and vertex mass fluxes are exchanged through the in-cell corner zone interfaces (e.g., A in Fig. 3). Requiring DeBar consistency (by which the advection would not perturb a constant velocity region), the vertex mass advection δm_{da} can be evaluated from the mass advection through the cell faces (see Benson [11, 12]). Here d, a are the donor and acceptor vertices (vertex 1 or 2 respectively in Fig. 4). The upstream-weighted velocity at the middle of the flux volume will be:

$$\mathbf{u}_f = \mathbf{u}_d + 0.5\left(1 - \frac{\delta m_{da}}{m_d}\right)\Delta \mathbf{u}_{12}^{red} \tag{10}$$

In Eq. (10) the reduced slope Δu_{12}^{red} is obtained by using Eq. (8) with the gradient limited to keep the extrapolated velocities inside the VIP. The momentum flux flowing from the corner volume of vertex d to vertex a will be $\delta m_{da}\mathbf{u}_f$.

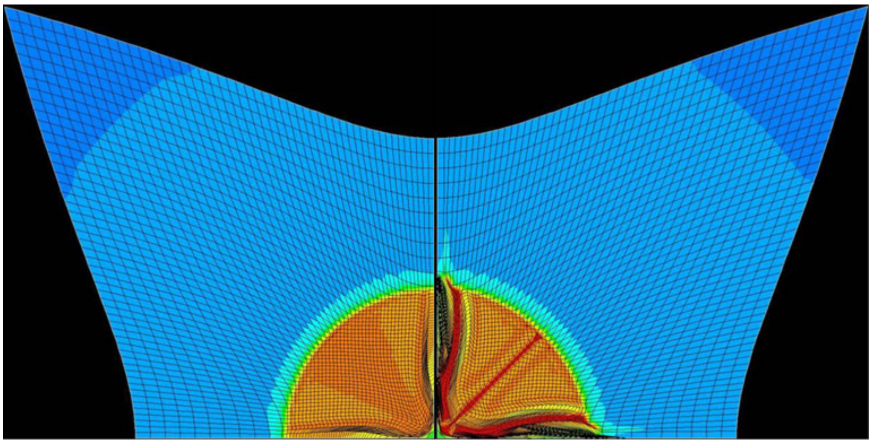

(a) VIP limiter (b) Component limiter

Fig. 5. 2D Noh Test isodensity at $T = 60$, Lagrangian.

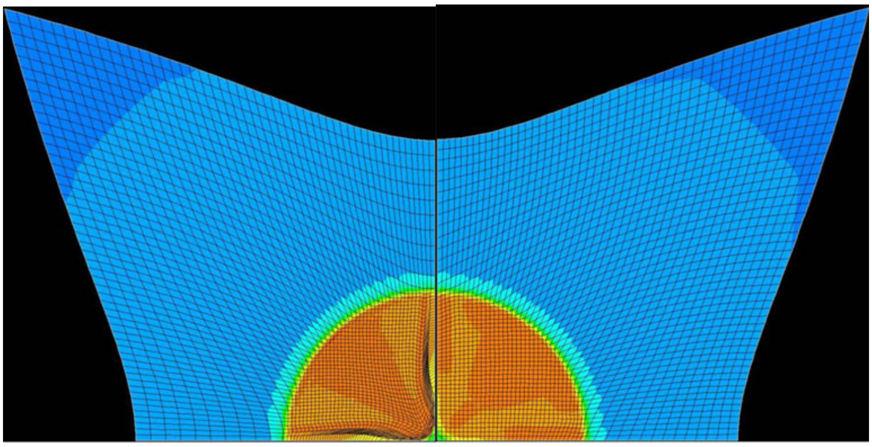

(a) VIP limiter, Lagrangian calculation (b) VIP limiter, ALE calculation

Fig. 6. 2D Noh Test isodensity at $T = 60$, Lagrangian and ALE.

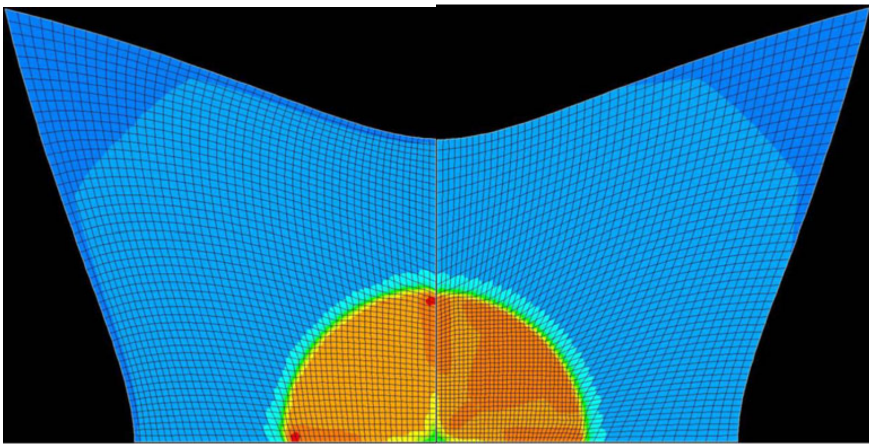

(a) VIP limiter, ALE more mesh smoothing (b) VIP limiter, ALE less mesh smoothing

Fig. 7. 2D Noh Test isodensity at $T = 60$, ALE.

6 Cylindrical (2D) Noh Test [15]

A cold ideal gas ($\gamma = 5/3, e = 0$) collapses radially with $[p, \rho, u_r] = [0, -1, 0]$, producing a strong outgoing shock propagating at speed $U_s = 1/3$. The exact solution is:

$$\rho(r) = \begin{cases} (1 + t/r) & t/3 < r < t \\ 16 & 0 \le r < t/3 \end{cases} \tag{11}$$

This problem is a challenging test for many schemes. Pseudo-viscosity can falsely add shock heating in regions of geometrically converging (smooth) flows. In the SMG scheme, the limiter serves also as a "shock detector" and helps prevent such false heating. When this test problem is set up with a Cartesian mesh, most Lagrangian schemes violate its cylindrical symmetry, producing severe mesh distortions that often force the calculation to stop.

In our test runs all calculations were performed until $t = 60$. The Lagrangian results in Fig. 5 demonstrate that the VIP limiter produces much less grid distortion than the previous component limiter (CL), as shown also in [1]. Of course with ALE mesh motion the grid distortion can be (almost) eliminated. In Fig. 6 we compare VIP and CL limiters for an ALE calculation, where the amount of mesh smoothing was just enough to prevent severe mesh distortion. Clearly, the density profile at $T = 60$ is more symmetric with the VIP limiter. In Fig. 7 we compare the previous VIP calculation with another VIP calculation where a larger degree of mesh smoothing was applied. It is evident that the reduced mesh motion calculation is the more symmetric one.

7 Conclusions

Compared to component limiters, the novel VIP limiter definitely improves symmetry preservation in the cylindrical Noh (ALE) test problem. Enhanced mesh smoothing, even with the VIP limiter, produces more symmetry violation near the symmetry planes. Hence the flux terms in the ALE advection phase might still have some symmetry-violating effect in this test problem.

References

1. G. Luttwak, J. Falcovitz, Int. J. Num. Meth. Fluids, (2010), published on-line, Wiley InterScience to appear in print.
2. G. Luttwak, J. Falcovitz, J. Energetic Materials, **28**, (2010), 279–302.
3. B. van Leer, J. Comput. Phys., **32**, (1979), 101–136.
4. M. Ben-Artzi, J. Falcovitz, *The Generalized Riemann Problem in Computational Fluid Dynamics*. Cambridge University Press, London, 2003.
5. M.J. Hubbard, J. Comput. Phys., **155**, (1999), 54–74.
6. W.J. Rider, D.B. Kothe, AIAA-972036, 1997.
7. M. Berger, M.J. Aftosmis, S.M. Murman, NASA Technical Report NAS-05-007, (2005).
8. J. O'Rourke, *Computational Geometry in C*. Cambridge University Press, London, 1998.
9. G. Luttwak, Shock Compression of Condensed Matter–2001, (M.D. Furnish et. al. Eds, AIP, CP620, 2002), 255–258.
10. G. Luttwak, J. Falcovitz, Shock Compression of Condensed Matter–2005, (M.D. Furnish et. al. Eds, AIP, CP845, 2006), 339–342.
11. D.J. Benson, J. Comput. Phys., **100**, (1992), 143–162.
12. D.J. Benson, Int. J. Num. Meth. Engineering, **75**, (2008), 1549–1580.
13. E.J. Caramana, M.J. Shashkov, R.P. Whalen, J. Comput. Phys., **144**, (1998), 70–97.
14. E.J. Caramana, D.E. Burton, M.J. Shashkov, R.P. Whalen, J. Comput. Phys., **146**, (1998), 227–262.
15. W.F. Noh, J. Comput. Phys., **72**, (1987), 78–120.